STAT-3 RNAscope Determination in Human Diffuse Large B-Cell Lymphoma[1]

Roberto Tamma [*], Giuseppe Ingravallo [†], Francesco Albano [‡], Francesco Gaudio [‡], Tiziana Annese [*], Simona Ruggieri [*], Loredana Lorusso [*], Mariella Errede [*], Eugenio Maiorano [†], Giorgina Specchia [‡] and Domenico Ribatti [*]

[*]Department of Basic Medical Sciences, Neurosciences, and Sensory Organs, University of Bari Medical School, Bari, Italy; [†]Department of Emergency and Transplantation, Pathology Section, University of Bari Medical School, Bari, Italy; [‡]Department of Emergency and Transplantation, Hematology Section, University of Bari Medical School, Italy

Abstract

BACKGROUND: Diffuse large B-cell lymphoma (DLBCL) is the most common form of non-Hodgkin's lymphoma. Signal transducer and activator of transcription 3 (STAT3) is a cytoplasmic transcription with many important functions, including regulation of cell proliferation, differentiation, survival, angiogenesis, and immune response. MATERIALS AND METHODS: In this study, we have compared by means of RNAscope technology STAT3 RNA expression in human DLBCL in a selected group of activated B-cell–like DLBCL (ABC-DLBCL) patients with another group of germinal center B-cell–like DLBCL (GBC-DLBCL) patients. RESULTS: The results have shown that ABC DLBCL tissue samples contained a significantly higher number of STAT3-positive cells as compared with GCB tissue samples. Moreover, by means of confocal immunofluorescence analysis, we have observed that tumor vessels in ABC samples appeared lined by endothelial cells expressing both FVIII and STAT3 signals, while in GCB samples, only few vessels coexpressed FVIII and STAT3. CONCLUSIONS: These data confirm other reports showing that STAT3 is highly expressed and activated in ABC-DLBCL and our previously published data demonstrating that, in primary central nervous system lymphoma, tumor vessels appeared lined by endothelial cells expressing both FVIII and STAT3.

Translational Oncology (2019) 12, 545–549

Introduction

Diffuse large B-cell lymphoma (DLBCL) is the most common form of non-Hodgkin's lymphoma (NHL), accounting for about 49% of B-cell cancers worldwide [1]. DLBCL presents a high clinical and biological heterogeneity due to the notion that most of these lymphomas arise from germinal center B-cells at different stages of differentiation, in which recurrent genetic alterations contribute to the molecular pathogenesis of the disease [2]. Based on their gene expression similarities either to normal germinal center (GC) B cells or in vitro–activated peripheral blood B cells, DLBCLs are classified in three groups, including the GC-B-cell–like DLBCL (GCB-DLBCL), activated B-cell–like DLBCL (ABC-DLBCL), and an unclassified third type [3]. The GCB group expresses high levels of BCL6 and responds better to conventional chemotherapy, whereas the ABC group has lower levels of BCL6 and tends to be refractory to chemotherapeutic treatment [4].

The Janus kinase (JAK) and signal transducer activator of transcription (STAT) pathways are involved in NHLs [5,6].

https://doi.org/10.1016/j.tranon.2018.12.008

Moreover, constitutively activated STAT3 is correlated with more advanced clinical stage and overall poor survival of DLBCL in humans [7,8]. Ding et al. [5] demonstrated that STAT3 gene is a transcriptional target of BCL6 and that STAT3 is highly expressed and activated in ABC-DLBCL and BCL6-negative normal germinal center B-cells. In this context, constitutive STAT3 activation represents a second oncogenic pathway in ABC-DLBCL providing an additional therapeutic target for treatment of these malignancies. Moreover, targeting the STAT pathway, which seems to be critical in tumorigenesis, is promising for multiple malignancies including lymphoma and leukemia.

RNAscope technology is a novel in situ hybridization (ISH) derived assay for detection of target RNA within intact cells. This assay is known for its sensitivity and specificity due to unique probe design strategy that allows simultaneous signal amplification and background suppression to achieve single-molecule visualization preserving tissue morphology. Moreover, its versatility allows it to be used by both fluorescence and visible approach [9].

In this study, we have compared by means of RNAscope technology STAT3 RNA expression in human DLBCL in a selected group of ABC patients with another group of GBC patients.

Materials and Methods

Patients

This retrospective study reviewed data from 30 patients diagnosed with DLBCL collected from the archive of the Section of Pathology of the University of Bari, Hospital Policlinico, Bari, Italy, between 2009 and 2013. All procedures were in accordance with the ethical standards of the responsible committee on human experimentation (institutional and national) and with the Helsinki Declaration of 1964 and later versions, and signed informed consent from individual patients was obtained to conduct the study. All patients had pathologically confirmed DLBCL. Tumors were divided into two histological subgroups: one that includes 15 ABC patients and another that includes 15 GCB patients.

STAT3 RNAscope Assay

RNAscope assay was performed on FFPE biopsies using RNAscope 2.5 HD Reagent Kit [RED 322360, Advanced Cell Diagnostics (ACD), Hayward, CA]. Briefly, tissue sections were deparaffinized with xylene and 100% ethanol and incubated with pretreat-1 solution for 10 minutes, pretreat-2 for 15 minutes, and pretreat-3 for 30 minutes (Pretreatment kit 322330, ACD). The slides were then hybridized with a probe Hs-STAT3 (ref. 425631), positive control probe: Hs-PPIB (ref. 313901), and negative control probe: DapB (ref. 310043) in the HybEZ oven (ACD) at 40°C for 2 hours. The Hs-PPIB probe for human housekeeping gene PPIB was used as a control to ensure RNA quality. After hybridizations, slides were subjected to signal amplification using HD 2.5 detection kit, and hybridization signal was detected using a mixture of Fast-RED solutions A and B (1:60). After counterstaining with Gill's hematoxylin, slides were dried in a 60°C dry oven for 15 minutes and mounted with Glycergel Mounting Medium (Dako, C0563). Sections from each experimental group were scanned using the whole-slide morphometric analysis scanning platform Aperio Scanscope CS (Leica Biosystems, Nussloch, Germany). All the slides were scanned at the maximum available magnification (40×) and stored as digital high-resolution images on the workstation associated with the

instrument. Based on the PPIB evaluation, all the cases were included in the analysis. Digital slides were inspected with Aperio ImageScope v.11 software (Leica Biosystems, Nussloch, Germany) at 20× magnification, and 10 fields with an equal area were selected for the analysis at 40× magnification. The mRNA expression was assessed by Aperio RNA ISH algorithm that provides standardized quantitation of RNA ISH staining in whole slide images of FFPE tissue. This algorithm automatically quantifies the staining across whole slides and counts individual molecular signals and clusters in the cells. The obtained results are divided in 3 ranges: 1+ that includes cells containing 2 to 5 dots for cell; 2+ that includes cells containing 6 to 20 dots for cell; 3+ that includes cells containing more than 20 dots for cell. The statistical significance of differences between the mean values of the percent labeled areas between ABC and GCB tumor specimens was determined by the two-way ANOVA test in GraphPad Prism 5.0 software (GraphPad Software, La Jolla, CA). Findings were considered significant at P values < .05.

FVIII and STAT3 Immunofluorescence

Since Fast Red produces a red reaction product detectable using either bright field or fluorescent microscopy, the same sections used in RNAscope assay were treated for FVIII immunofluorescence in order to evaluate the coexpression of STAT3 mRNA and FVIII protein. The slides used in RNAscope assay have been disassembled by incubation at 60°C in an oven for few minutes. Afterwards, slides were washed in PBS and processed by immunofluorescence classical protocol. The sections were incubated for 30 minutes in a blocking buffer [BB; phosphate-buffered saline (PBS), pH 7.4, 1% bovine serum albumin, 2% fetal calf serum] and exposed to primary antibody rabbit anti-FVIII (A0082, Dako) diluted 1:50 in BB overnight at 4°C. After washing in PBS, the sections were incubated for 2 hours with the secondary antibody Alexa Fluor 555 goat anti-rabbit antibodies (Invitrogen) and diluted 1:300 in BB. All the samples were incubated for 20 minutes with 0.01% TO-PRO-3 (Invitrogen) for nuclear staining and mounted in Vectashield (Vector Laboratories Inc., Burlingame, CA). Negative controls, obtained by substituting primary antibodies with specific preimmune serum (Dako), showed no staining of the sections. The sections were examined under a Leica TCS SP5 (Leica, Wetzlar, Germany) confocal laser scanning microscope using 40× and 63× objective lenses with either 1× or 2× zoom factors. A sequential scan procedure was applied during image acquisition of the two fluorophores. Confocal images were taken at 0.3-mm intervals through the z-axis of the section covering a total depth of 10 μm. Images from individual optical planes and multiple serial optical sections were analyzed, digitally recorded, and stored as TIFF files using Adobe Photoshop software (Adobe Systems Inc., San Jose, CA). Morphometric analysis was performed by two independent observers on 10 randomly selected fields observed at 63× magnification by using Cell^F as image analysis software (Olympus Italia, Rozzano, Italy). STAT3/FVIII-positive vessels (red signal: STAT3 and green signal: FVIII) were evaluated, and the results were presented as percentage area with coexpression of STAT3 and FVIII. The data were expressed as mean value ± SD.

Results

RNAscope-STAT3 Expression

RNAscope assay was performed in order to evaluate the expression of STAT3 mRNA in tumor cells in both ABC and GCB groups of
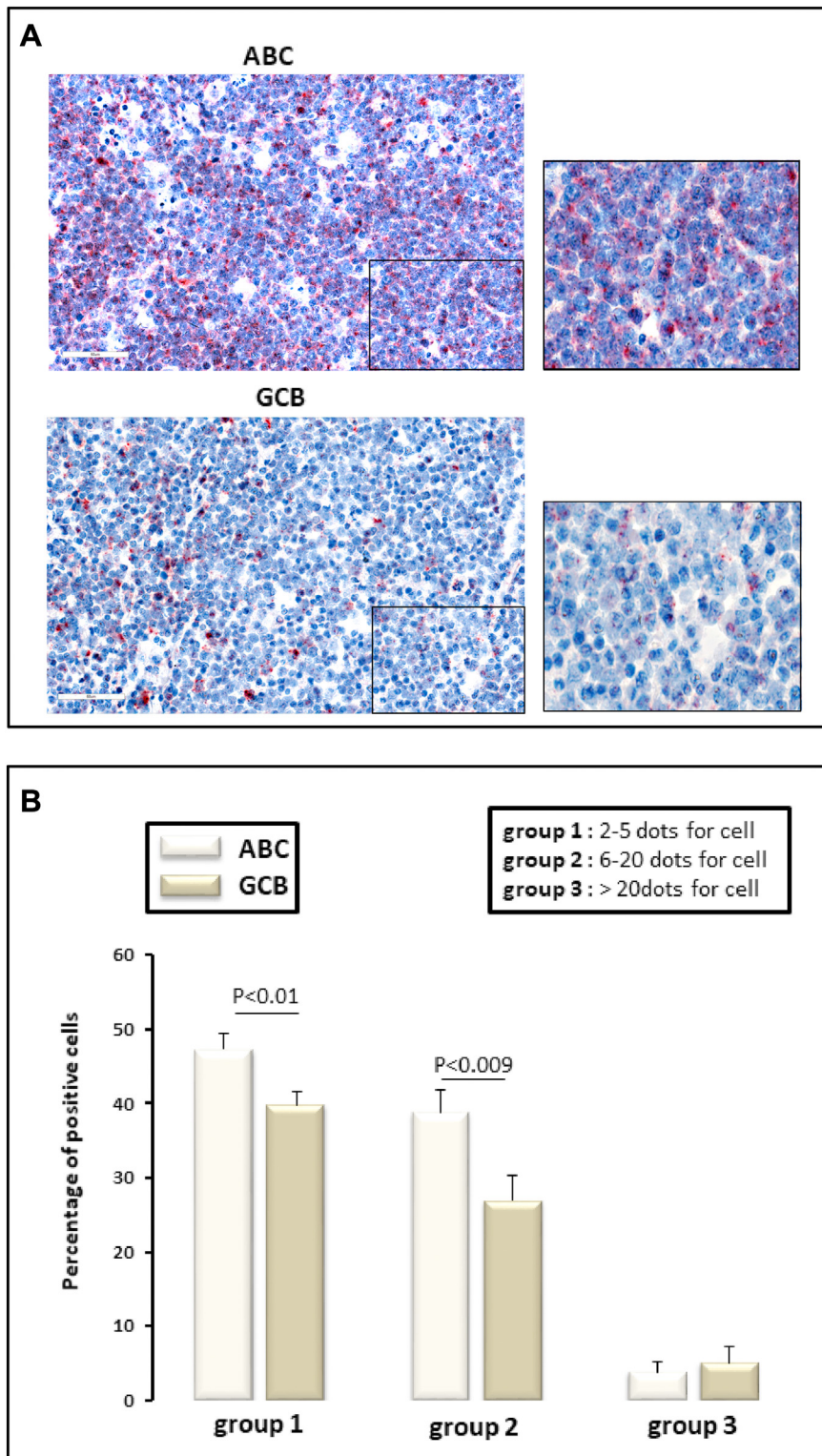
Figure 1. (A) RNAscope-STAT3 mRNA expression in histological samples of ABC and GCB DLBCL experimental groups (inset at higher magnification). Scale bar: 60 μm. (B) Quantitation of RNA ISH staining of STAT3 mRNA positivity in ABC and GCB DLBCL samples. The percent of STAT3 mRNA expression significantly increases in the ABC group 1 and 2 tumor samples compared to GCB.

DLBCL tissue samples (Figure 1A). Three groups of data have been considered according to the number of STAT3-positive signals (red dots) contained in each cell. Group 1 included the percentage of cells containing from 2 to 5 dots, group 2 included the percentage of cells containing from 6 to 20 dots, and group 3 included the percentage of cells containing more than 20 dots. ABC tissue samples contained a significant higher number of positive cells in both group 1 and 2 as compared to GCB tissue samples. A low number of cells belonging to the group 3 have been observed in all the tissue samples, and no significant differences in their number between the ABC and GCB
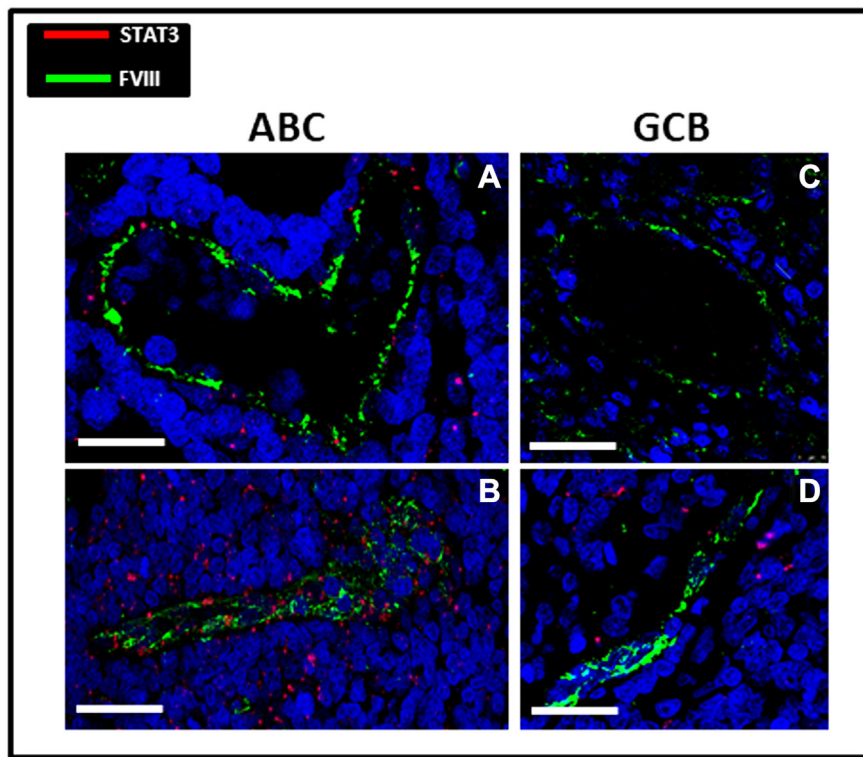
Figure 2. STAT3 (red)/FVIII (green) confocal fluorescence/immunofluorescence evaluation in ABC (A, B) and GCB (C, D) DLBCL histological samples. ABC vessels are lined by endothelial cells expressing FVIII and Stat3 fluorescence signals (A, B). Vessels from GCB group show only the FVIII signal (B, C). Scale bar (A) 22.5 μm, (B) 40.2 μm, (C) 37.5 μm, and (D) 26.5 μm.

experimental groups have been seen. Figure 1B shows morphometric analysis of the STAT3 expression in ABC/group 1 (47.4% ± SE 2%), ABC/group 2 (38.7% ± SE 3.1%), and ABC/group 3 (4.0% ± SE 1.4%) as compared with GCB/group 1 (39.8% ± SE 1.8%), GCB/group 2 (26.9% ± SE 0.18%), and GBC/group 3 (5% ± SE 2.3%).

Confocal Microscopy-FVIII/STAT3 Expression

After confocal immunofluorescence reactions, tumor vessels in ABC samples appeared lined by endothelial cells expressing both FVIII and STAT3 signals (Figure 2, A and B), while in GCB samples, only few vessels coexpressing FVIII and STAT3 were detectable (Figure 2, C and D). Morphometric analysis showed that the STAT3/FVIII coexpressing cells were significantly higher in ABC samples (0.15% ± SE 0.02%) as compared to GBC ones (0.056% ± SE 0.01%) (Figure 3A). The percentage of STAT3-positive cells was significantly higher in ABC samples (3.32% ± SE 0.6%) as compared to GBC ones (0.83% ± SE 0.2%), while no significant differences were recognizable as concerns FVIII positivity in ABC (2.06% ± SE 0.56%) and GCB (2.11% ± SE 0.34%) groups (Figure 3B).

Discussion

The results of this study performed by means of RNAscope technology have shown that ABC DLBCL tissue samples contained a significantly higher number of STAT-3–positive cells as compared with GCB tissue samples. Moreover, by means of confocal immunofluorescence analysis, we have observed that tumor vessels in ABC samples appeared lined by endothelial cells expressing both FVIII and STAT3 signals, while in GCB samples, only few vessels coexpressed FVIII and STAT3.

Activated STAT3 promotes tumor cell proliferation and survival, immune suppression, invasion, and angiogenesis [10]. STAT3 is strongly linked to tumor angiogenesis and metastasis [11] and is related to poor prognosis in different tumors [12]. Hypoxia and inflammatory factors activate STAT3 to promote tumor angiogenesis. Persistent activation of STAT3 contributes to hypoxia inducible factor 1 alpha (HIF-1α) and vascular endothelial growth factor (VEGF) expression in cancer cells and other nonendothelial cells. VEGF then activates STAT3 in endothelial cells and promotes cell proliferation, migration, and survival. In addition, STAT3 inhibits the expression of tumor suppressors, such as the antiangiogenesis transcription factor p53 [13]. Antitumor effects of STAT-3 knockdown have been demonstrated by means of small interfering RNA (siRNA), micro-RNA (mi-RNA), or small molecule inhibitors [14,15]. Inhibition of the STAT3 signaling is a potential therapeutic strategy for tumor and other angiogenesis-related diseases [16].

RNAscope represents a significant improvement in RNA ISH methodology and is compatible with clinical sample types and laboratory workflows. The utilization of this highly sensitive method for oligonucleotide detection offers significant promise as a new platform for developing and implementing RNA-based molecular diagnostics useful when immunohistochemistry (IHC) is not available or when there is a difficulty in standardizing immunohistochemical analysis. Moreover, the combination of mRNA analysis through ISH and protein analysis through IHC in the same section could be an extremely powerful technique that allows to identify specific cell populations.

The results of this study confirm literature data showing that STAT3 gene is a transcriptional target of BCL6 and that STAT3 is highly expressed and activated in ABC-DLBCL and BCL6-negative normal germinal center B cells [5]. Moreover, more recently, it has been demonstrated that DLBCL initiates dissemination through activating STAT3-mediated amoeboid migration [17].
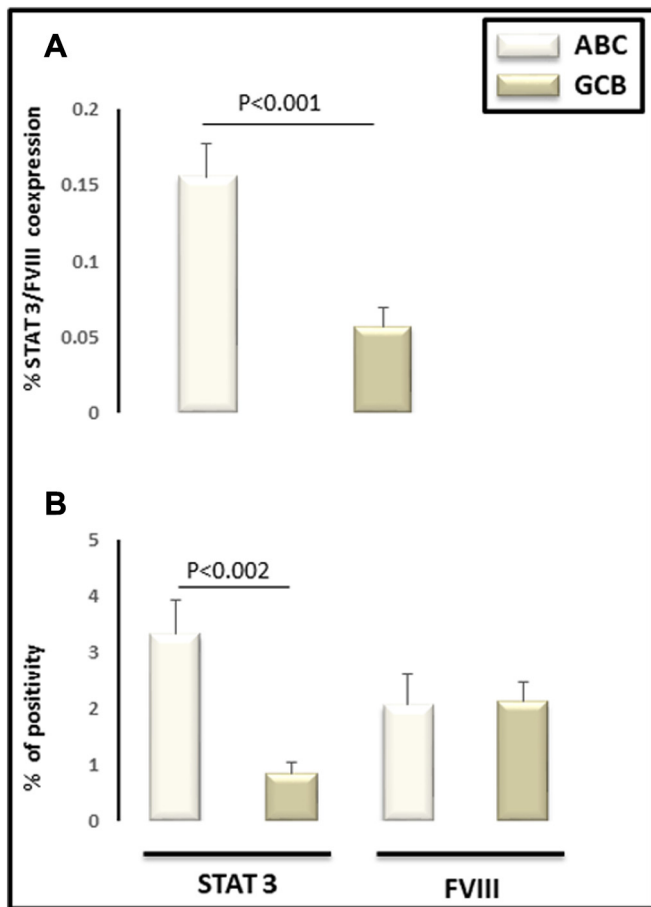
Figure 3. Morphometric analysis of STAT3 and FVIII expression showing a significantly increased coexpression of STAT3 and FVIII in vessels of ABC group compared with GCB one (A). Fluorescence evaluation of STAT3 expression shows its higher expression in ABC group respect to GCB (B). FVIII is equally expressed in all the experimental groups (B).

These data confirm also our previously published data showing that, in primary central nervous system lymphoma, tumor vessels appeared lined by endothelial cells expressing both FVIII and STAT3 signals, while in the control brain tissue, only FVIII-positive vessels were detectable [18]. Endothelial cells lining these vessels are heterogeneous, expressing FVIII and STAT3, and presumably, originally they are vascular progenitor cells. Interestingly, it is to note that STAT3 is required for the maintenance of pluripotency in murine stem cells [19].

Acknowledgements

References

[1] Campo E, Swerdlow SH, Harris NL, Pileri S, Stein H, and Jaffe ES (2011). The 2008 WHO classification of lymphoid neoplasms and beyond: evolving concepts and practical applications. *Blood* **117**, 5019–5032.

[2] Schneider C, Pasqualucci L, and Dalla-Favera R (2011). Molecular pathogenesis of diffuse large B-cell lymphoma. *Semin Diagn Pathol* **28**, 167–177.

[3] Alizadeh AA, Eisen MB, Davis RE, Ma C, Lossos IS, Rosenwald A, Boldrick JC, Sabet H, Tran T, and Yu X, et al (2000). Distinct types of diffuse large B-cell lymphoma identified by gene expression profiling. *Nature* **403**, 503–511.

[4] Rosenwald A, Wright G, Chan WC, Connors JM, Campo E, Fisher RI, Gascoyne RD, Muller-Hermelink HK, Smeland EB, and Giltnane JM, et al (2002). The use of molecular profiling to predict survival after chemotherapy for diffuse large-B-cell lymphoma. *N Engl J Med* **346**, 1937–1947.

[5] Ding BB, Yu JJ, Yu RYL, Mendez LM, Shaknovich R, Zhang Y, Cattoretti G, and Ye BH (2007). Constitutively activated STAT3 promotes cell proliferation and survival in the activated B-cell subtype of diffuse large B-cell lymphomas. *Blood* **111**, 1515–1523.

[6] Alas S and Bonavida B (2003). Inhibition of constitutive STAT3 activity sensitizes resistant non-Hodgkin's lymphoma and multiple myeloma to chemotherapeutic drug-mediated apoptosis. *Clin Cancer Res* **9**, 316–326.

[7] Ok CY, Chen J, Xu-Monette ZY, Tzankov A, Manyam GC, Li L, Visco C, Montes-Moreno S, Dybkaer K, and Chiu A, et al (2014). Clinical implications of phosphorylated STAT3 expression in de novo diffuse large B-cell lymphoma. *Clin Cancer Res* **20**, 5113–5123.

[8] Zl W, Yq S, Yf S, and Zhu J (2011). High nuclear expression of STAT3 is associated with unfavorable prognosis in diffuse large B-cell lymphoma. *J Hematol Oncol* **4**, 31.

[9] Wang F, Flanagan J, Su N, Wang LC, Bui S, Nielson A, Wu X, Vo HT, Ma XJ, and Luo Y (2012). RNAscope: a novel in situ RNA analysis platform for formalin-fixed, paraffin-embedded tissues. *J Mol Diagn* **14**, 22–29.

[10] Kim J, Patel M, Ruzevick J, Jackson C, and Lim M (2014). STAT3 activation in glioblastoma: biochemical and therapeutic implications. *Cancer* **6**, 376–395.

[11] Doucette TA, Kong L-Y, Yang Y, Ferguson SD, Yang J, Wei J, Qiao W, Fuller GN, Bhat KP, and Aldape K, et al (2012). Signal transducer and activator of transcription 3 promotes angiogenesis and drives malignant progression in glioma. *Neuro Oncol* **14**, 1136–1145.

[12] Yu H, Kortylewski M, and Pardoll D (2007). Crosstalk between cancer and immune cells: role of STAT3 in the tumour microenvironment. *Nat Rev Immunol* **7**, 41–51.

[13] Gao P, Niu N, Wei T, Tozawa H, Chen X, Zhang C, Zhang J, Wada Y, Kapron CM, and Liu J (2017). The roles of signal transducer and activator of transcription factor 3 in tumor angiogenesis. *Oncotarget* **8**, 69139–69161.

[14] Ashizawa T, Miyata H, Iizuka A, Komiyama M, Oshita C, Kume A, Nogami M, Yagoto M, Ito I, and Oishi T, et al (2013). Effect of the STAT3 inhibitor STX-0119 on the proliferation of cancer stem-like cells derived from recurrent glioblastoma. *Int J Oncol* **43**, 219–227.

[15] Li GH, Wei H, Lv SQ, Ji H, and Wang DL (2010). Knockdown of STAT3 expression by RNAi suppresses growth and induces apoptosis and differentiation in glioblastoma stem cells. *Int J Oncol* **37**, 103–110.

[16] Herbert SP and Stainier DYR (2011). Molecular control of endothelial cell behaviour during blood vessel morphogenesis. *Nat Rev Mol Cell Biol* **12**, 551–564.

[17] Pan Y-R, Chen C-C, Chan Y-T, Wang H-J, Chien F-T, Chen Y-L, Liu J-L, and Yang M-H (2018). STAT3-coordinated migration facilitates the dissemination of diffuse large B-cell lymphomas. *Nat Commun* **9**, 3696.

[18] Ruggieri S, Tamma R, Resta N, Albano F, Coccaro N, Loconte D, Annese T, Errede M, Specchia G, and Senetta R, et al (2017). Stat3-positive tumor cells contribute to vessels neoformation in primary central nervous system lymphoma. *Oncotarget* **8**, 31254–31269.

[19] Niwa H, Burdon T, Chambers I, and Smith A (1998). Self-renewal of pluripotent embryonic stem cells is mediated via activation of STAT3. *Genes Dev* **12**, 2048–2060.